

Supplemental Table and Figure Legends:

Table S1, related to Figure 1. Data collection and refinement statistics for the 5 structures solved in this study.

Table S2, related to Table 1. V D and J gene segment usage and junctional sequences of the TCRs used in this study as well as other notable I-Ek reactive TCRs. For each TCR, the $V\alpha$ gene name, CDR3 α sequence, $J\alpha$ gene name, $V\beta$ gene name, CDR3 β sequence, $J\beta$ gene name and peptide specificity is listed. IMGT nomenclature is used for all TCR gene names. In addition to 2B4 and 226 TCRs, crystallized in this study, the 5c.c7 and AND TCR sequences are shown for comparison purposes as they are widely studied MCC/I-Ek reactive TCRs. The 202 TCR shares the same β chain as 226 and 5c.c7 and reacts with only MCC-p5E not wildtype MCC. The E21 TCR shares the same α chain as 5c.c7 but reacts only with MCC-p8E not wildtype MCC. It is interesting to note that this TCR uses the $V\beta 8.2$ gene segment, for which there is a great deal of structural information.

Figure S1, related to Figure 3. Contact surfaces for each loop and inter-residue contacts.

(A) Here the pMHC residues bound by each CDR loop of the 2B4 and 226 TCR are highlighted for each CDR loop of each TCR chain. The upper plots show the residues bound by CDR1, CDR2, HV4 and CDR3 loops of both 2B4 α and 226 α . Underneath the only CDR2 and CDR3 made pMHC contacts from 2B4/226 β . For each, residues colored in blue make contact in all three structures. Magenta indicates residues only contacted by

2B4. Cyan residues are contacted only by 226 in the p5K structure. Green residues make contacts with 226 in both the p5K and p5E structures. Red residues are contacted by both the 2B4 and 226 TCRs bound to MCC-p5K/I-E^k. **(B, C)** To illustrate the similarity in docking of Inter-residue contacts between the CDR1, CDR2 and HV4 loops of 2B4 α and I-E^k β **(B)** or CDR2 of 2B4 β and I-E^k α **(C)** are illustrated. As in Figure 3, lines connecting each residue represent van der Waals interactions (black), hydrogen bonds (red) and salt-bridges (blue). For comparison purposes, the contacts between 1934.4 TCR CDR1 and 2 α , and sequence-aligned I-A^u β are shown in panels B and C.

Figure S2, related to Figure 3. Summary of functional data and its relationship to the 2B4 and 226 complex crystal structures. **(A)** This panel summarizes mutational data, where Ala or Gly mutations were made in I-E^k as well as various MCC peptide mutations (Wu et al.). Each residue is colored by its effect on 2B4 TCR binding as measured by SPR where grey indicates a less than 3 \times decrease in steady-state affinity, pink indicates a 3–100 \times decrease and red indicates a greater than 100 \times decrease in steady-state affinity. **(B)** This panel summarizes functional data using a peptide dose-response curve for IL-2 cytokine production as a read-out for 2B4 hybridoma T cell activation using CHO cells expressing wild-type or mutant I-E^k as APCs for wild-type or mutant MCC peptides. In this panel grey indicates a less than 20 \times change in the EC50 for peptide elicited IL-2 production, pink indicates a 20–100 \times increase in EC50 for IL-2 production and red indicates a greater than 100 \times increase in peptide EC50 for IL-2 production (Ehrich et al., 1993; Reay et al., 1994). **(C)** Here each of the peptide and I-E^k residues tested are colored according to their measured phi value, a measurement of the contribution of the residue

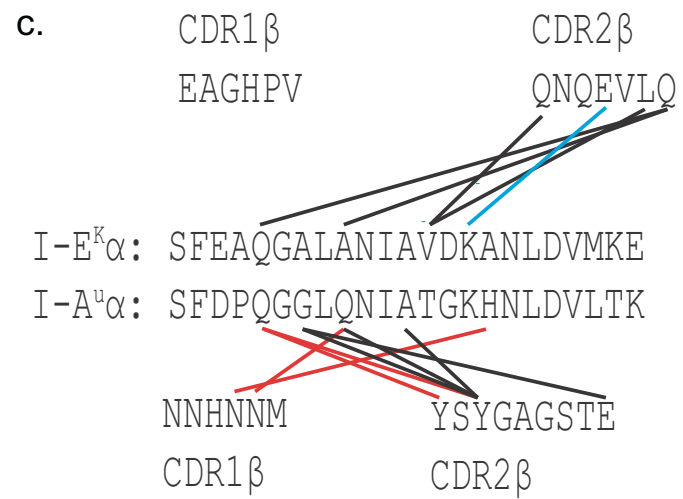
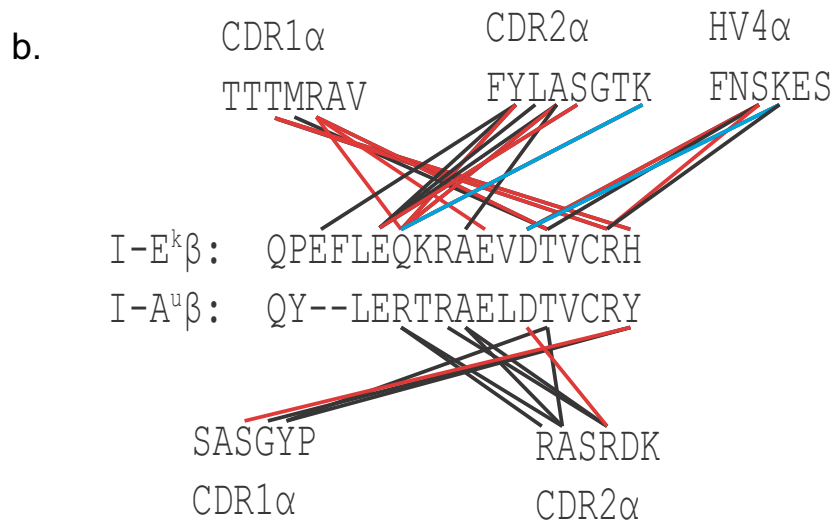
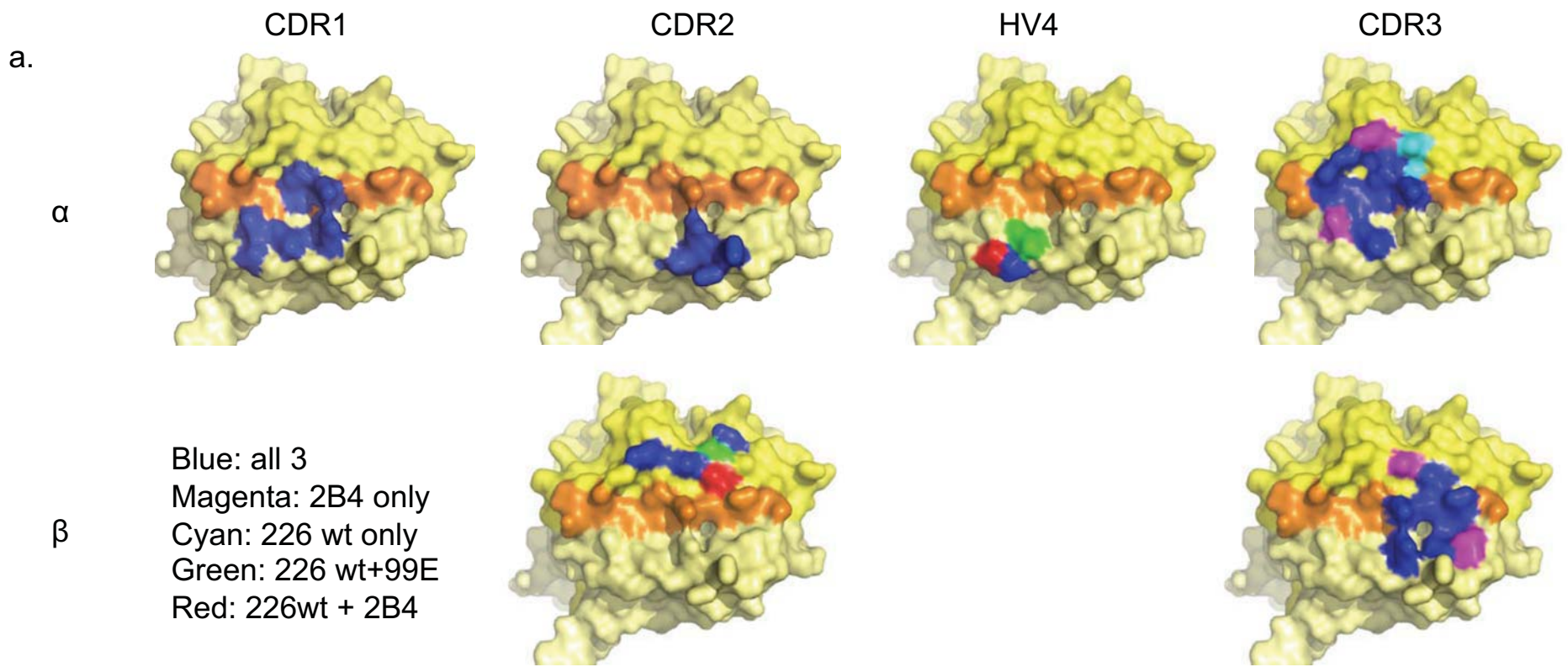
to the 2B4 TCR binding transition state. Residues colored grey were tested but had insignificantly small phi values, pink represents a significant phi value that is less than 0.3 and residues colored red have significant phi values greater than 0.3 (Wu et al.). **(D, E)** Alterations in stimulatory capacity of mutant I-E^k molecules expressed in CHO cells for 226, using MCC (D) or MCC-p5E (E) as a stimulatory peptide. In this panel, mutants of residues colored gray caused a less than 20× change in peptide potency for IL-2 production, mutants of residues colored pink caused a 20–100× increase in peptide EC50 and mutants of red residues caused a greater than 100× decrease in peptide potency. Green residues represent mutations that actually improved the peptide stimulatory capacity of MCC (D) or MCC-p5E (E) peptide with a 20–100× decrease in peptide EC50.

Table S1. Data collection and refinement statistics

	2B4-MCC/I-E^k	226-MCC/I-E^k	226-MCC-p5E/I-E^k	2B4	5c.c7
Data collection					
Space group	F 222	P 2 ₁	P 2 ₁	P 6 ₅ 22	P 2 ₁ 2 ₁ 2
Cell dimensions					
<i>a</i> , <i>b</i> , <i>c</i> (Å)	147, 167, 259	72.8, 71.4, 106	72.2, 71.6, 106	93.9, 93.9, 389	133, 139, 62.0
α , β , γ (°)	90.0, 90.0, 90.0	90.0, 90.8, 90.0	90.0, 90.0, 90.0	90, 90, 120	90, 90, 90
Resolution (Å)	2.7	2.7	3.3	2.4	1.9
R _{merge}	8.1 (48.5)	9.6 (46.4)	10.2 (34.5)	14.6 (85.6)	4.1 (26.7)
<i>I</i> / σI	14.4 (2.1)	6.9 (1.7)	10.7 (3.0)	13.0 (3.4)	20.2 (4.5)
Completeness (%)	99.4 (95.4)	100 (100)	98.4 (99.4)	99.6 (99.3)	99.6 (98.9)
Redundancy	3.8 (3.3)	5.1 (5.2)	3.2 (3.2)	14.3 (14.6)	3.7 (3.7)
Refinement					
Resolution (Å)	35–2.7	37–2.7	37–3.3	47–2.4	46–1.9
No. reflections	43476	30135	16244	40595	174859
R _{work} / R _{free}	22.1/ 24.6	21.5/ 25.4	21.9/ 26.5	20.9/ 25.9	22.3/ 25.5
No. atoms					
protein	6221	6252	6234	6823	6830
carbohydrate	59	28	28	-	-
water	108	99	-	224	388
PEG	49	-	-	-	-
R.m.s. deviations					
Bond length (Å)	0.010	0.003	0.005	0.010	0.007
Bond angles (°)	1.30	0.70	0.82	1.16	1.03
average B-factor (Å ²)	54.6	47.3	62.8	39.2	32.2
Ramachandran (% favored, allowed, generously allowed, disallowed)	88.5, 11.3, 0.1, 0.0	89.5, 10.0, 0.4, 0.0	88.8, 10.8, 0.4, 0.0	89.9, 9.7, 0.4, 0.0	89.5, 10.2, 0.3, 0.0

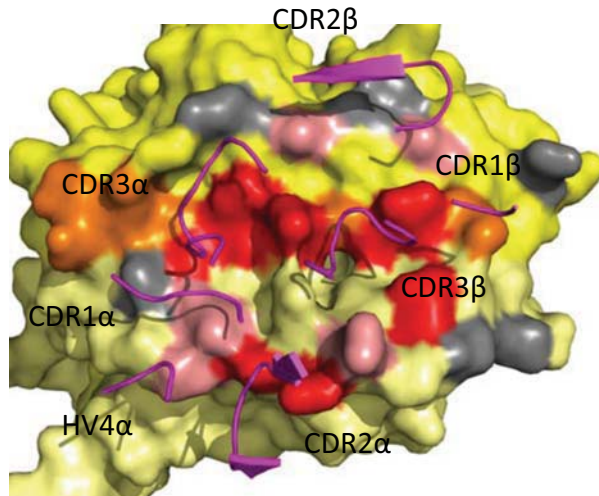
Table S2. V, D, J and CDR3s of MCC- and other peptide-I-E^k reactive TCRs

TCR	V α	CDR3 α	J α	V β	CDR3 β	J β	Peptide specificity
2B4	TRAV4D-4*2 (V α 11.2)	CAALRATGGNNKLT	TRAJ56	TRBV26 (V β 3)	CASSLNWSQDTQYF	TRBJ2.5 (D2)	MCC
5c.c7	TRAV4D-4*3 (V α 11.1)	CAAEASNTNKVVF (5c.c7 α)	TRAJ34	TRBV26 (V β 3)	CASSLNNANSDYTF (5c.c7 β)	TRBJ1.2 (D1)	MCC
226	TRAV4D-4*3 (V α 11.1)	CAAEPSSGQKLVF	TRAJ16	TRBV26 (V β 3)	CASSLNNANSDYTF (5c.c7 β)	TRBJ1.2 (D1)	MCC and MCC-99E
AND	TRAV4D-4*3 (V α 11.1)	CAAEASSGQKLVF	TRAJ16	TRBV26 (V β 3)	CASSLNNANSDYTF (5c.c7 β)	TRBJ1.2 (D1)	MCC
202	TRAV4D-4*3 (V α 11.1)	CAAKSSGSWQLIF	TRAJ22	TRBV26 (V β 3)	CASSLNNANSDYTF (5c.c7 β)	TRBJ1.2 (D1)	MCC-99E
E21	TRAV4D-4*3 (V α 11.1)	CAAEASNTNKVVF (5c.c7 α)	TRAJ34	TRBV13-2 (V β 8.2)	CASGENRSGNTLYF	TRBJ1.3 (D1)	MCC-102E
3L.2	TRAV8D-2*2 (V α 15)	CATTSGGNYKPTF	TRAJ6	TRBV13-1 (V β 8.3)	CASSGAGGAGTGQLYF	TRBJ1.1 (D1)	Hb



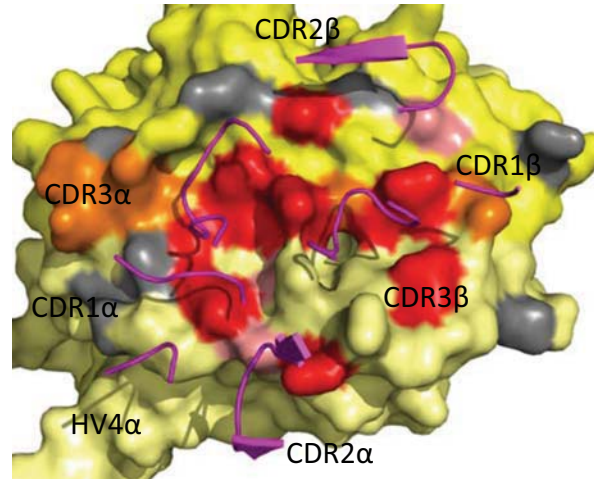
Supplementary Figure 1

a. 2B4 binding data



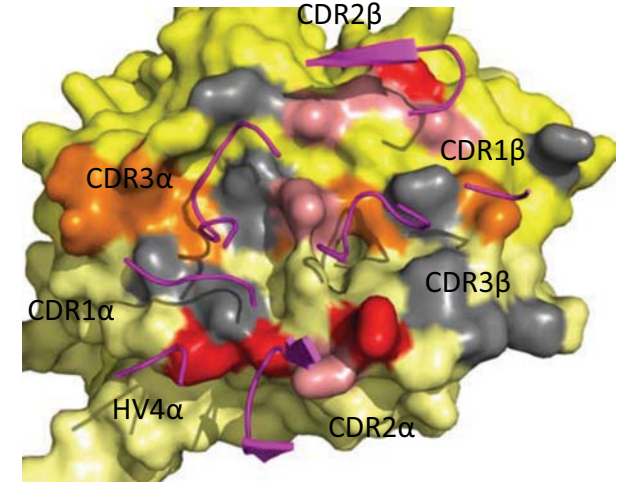
Red affinity >100 μM
Pink >3x reduction in affinity
Grey <3x reduction in affinity

b. 2B4 stimulation data



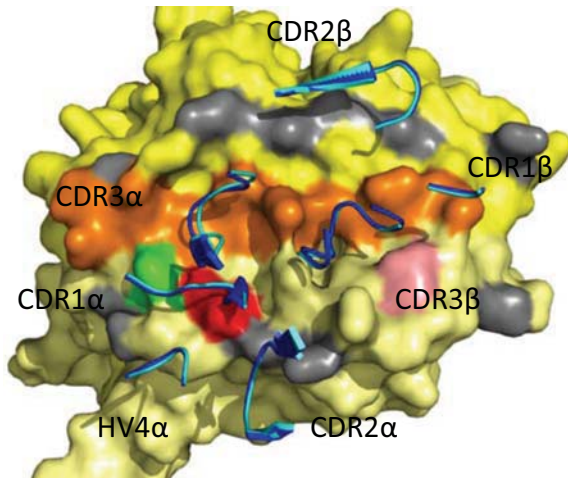
Gray no change
Pink 20–100x increase in EC50
Red >100x increase in EC50

c. I-E^k 2B4 phi data



Red phi >0.3
Blue phi sig <0.3
Gray NS phi measured

d. 226 stimulation MCC data



Gray no change
Pink 20–100x increase in EC50
Red >100x increase in EC50
Green decrease EC50

e. 226 stimulation p5E data

